Accepted Manuscript

Peptide cleavage-based electrochemical biosensor coupling graphene oxide and silver nanoparticles

Fanyu Meng, Haixuan Sun, Yue Huang, Yuguo Tang, Qiang Chen, Peng Miao

PII: S0003-2670(18)31146-2

DOI: 10.1016/j.aca.2018.09.053

Reference: ACA 236289

To appear in: *Analytica Chimica Acta*

Received Date: 16 May 2018

Revised Date: 15 September 2018

Accepted Date: 21 September 2018

Please cite this article as: F. Meng, H. Sun, Y. Huang, Y. Tang, Q. Chen, P. Miao, Peptide cleavage-based electrochemical biosensor coupling graphene oxide and silver nanoparticles, *Analytica Chimica Acta* (2018), doi: https://doi.org/10.1016/j.aca.2018.09.053.

A peptide cleavage-based strategy is developed for detection of prostate specific antigen.

Graphene oxide and silver nanoparticles are constructed for signal generation.

Significant silver stripping peak is used to evaluate prostate specific antigen concentration.

Peptide cleavage-based electrochemical biosensor coupling graphene oxide and silver nanoparticles

Fanyu Meng[a,b,†], Haixuan Sun[a,†], Yue Huang[c], Yuguo Tang[a], Qiang Chen[d,*], Peng Miao[a,*]

[a] Suzhou Institute of Biomedical Engineering and Technology, Chinese Academy of Sciences, Suzhou 215163, People's Republic of China

[b] University of Science and Technology of China, Hefei 230026, People's Republic of China

[c] College of Light Industry and Food Engineering, Nanjing Forestry University, Nanjing 210037, People's Republic of China

[d] the Key Laboratory of Bioactive Materials, Ministry of Education, College of Life Science, Nankai University, Tianjin 300071, People's Republic of China

[†] These authors contributed equally.

[*] Corresponding authors. E-mail: miaopeng@sibet.ac.cn (P. Miao); qiangchen@naikai.edu.cn (Q. Chen)

ABSTRACT

Herein, a novel electrochemical biosensor for sensitive analysis of prostate specific antigen (PSA) is demonstrated. A specific peptide is employed on the gold electrode as a molecular recognition element for target induced cleavage. In the absence of PSA, graphene oxide (GO) is directly immobilized on the peptide modified electrode, which triggers the aggregation of silver ions and subsequent reduction reaction to form silver nanoparticles (AgNPs). Well defined sharp silver stripping peak can thus be achieved, which stands for a highly characteristic solid-state Ag/AgCl reaction. However, in the presence of PSA, the peptide is specifically recognized and cleaved. The resulted product on the electrode surface cannot aid the immobilization of GO and subsequent formation of AgNPs. Therefore, electrochemical response is decreased remarkably, which can be used to indicate the concentration of PSA. This work demonstrates that the combination of the transduction of peptide cleavage event with GO/AgNPs nanocomposites is a promising attempt for PSA analysis with high sensitivity and selectivity.

KEYWORDS: prostate specific antigen; peptide; biosensor; graphene oxide; silver nanoparticles; linear sweep voltammetry.

1. Introduction

Prostate specific antigen (PSA) is a serine protease with chymotrypsin-like enzymatic activity, which is secreted by both normal prostate glandular cells and prostate cancer cells [1, 2]. PSA has long been identified as the best available biomarker for the screen of prostate cancer [3, 4]. Since early and precise evaluation of tumor biomarker enables improved therapeutic intervention, advanced methods for the analysis of PSA are in urgent need [5]. In the diagnostic of prostate cancer, the PSA cutoff value is up to 4.0 ng mL^{-1}, and higher concentration is warning threshold of prostate cancer [6]. For the monitoring of post-surgery recurrence of prostate cancer, the determination of PSA in low pg mL^{-1} region is required [7]. Therefore, development of ultrasensitive methods for the detection of trace PSA is of great interest for clinical and biological applications.

The determination of PSA has been routinely performed based on immunological recognition with techniques of colorimetry [8], fluorescence [9], surface-enhanced Raman scattering [10], electrochemistry [11], electrochemiluminescence [12], and so on. PSA specific aptamers with high binding affinity have also been applied for sensitive detection, which have certain merits over traditionally used antibodies like flexible design, convenient signal labeling and high extendibility [13]. Although these methods exhibit high sensitivity, the preparation or modification of these recognition elements may involve complicated processes. They may also be inactivated or unstable in real samples like blood. Therefore, alternative recognition elements should be explored and the development of novel PSA assays is still highly desired.

Recently, specific binding peptides have emerged as a more compelling choice for target recognition in bioassays with the advantages like facile production, high reliability and stability

[14, 15]. Peptides are also more amenable at the molecular level [16]. Various peptide-based biosensors have been developed for explosive analysis [17], apoptotic cells assay [18], juvenile idiopathic arthritis diagnosis [19], and so on. Since many peptides are natural substrates of proteases, by monitoring the specific cleavage events, the level of proteases can be determined [20]. PSA is a type of protease, which is suitable to be determined by the assessment of the cleavage activity of certain substrate peptide. Several peptide-based methods have already been developed for the detection of PSA. For example, Denmeade et al. identified a highly specific peptide containing the amino acid sequence HSSKLQ for PSA. By employing fluorescently tagged substrates, the enzymatic activity of PSA in extracellular fluids is determined [21]. However, intrinsic limitations on response sensitivity and complex synthesis and labeling processes prompt us to develop a more efficient peptide-based method for PSA evaluation.

In this contribution, we have developed a novel peptide cleavage-based electrochemical PSA biosensor. By analysis the electrochemical response from the nanocomposites of graphene oxide (GO) and silver nanoparticles (AgNPs), the concentration of PSA is determined. This sensing platform is highly sensitive, selective and have great potential practical utility.

2. Experimental

2.1 Materials and reagents

4-(2-hydroxyerhyl)piperazine-1-erhanesulfonic acid (HEPES), trisodium citrate, tris(2-carboxyethyl)-phosphine hydrochloride (TCEP), silver nitrate ($AgNO_3$), mercaptohexanol (MCH), bovine serum albumin (BSA), human alpha fetoprotein (AFP), and carcinoembryonic antigen (CEA) were purchased from Sigma (USA). GO was obtained from Nanjing XFNANO Materials Tech Co., Ltd (Nanjing, China). Peptides were synthesized and purified by China

Peptides Co., Ltd. (Shanghai, China). The sequence of the specific peptide was CGGHSSKLQFWYFWY. A random peptide sequence was also employed as a control (FNFRLKAGAKIRFGRGC). PSA was obtained from Shanghai Linc-Bio Science Co. LTD (Shanghai, China). 0.1 M phosphate buffered solution (PBS, pH 7.0) was prepared containing 0.1 M Na_2HPO_4, 0.1 M KH_2PO_4 and 0.1 M KCl. Human serum samples were acquired from Suzhou Science and Technology Town Hospital (Suzhou, China). All other chemicals were of reagent grade and used as received. Double-distilled water used to prepare all solutions was purified with a Millipore system under 18 MΩ·cm resistivity.

2.2 Peptide modified working electrode

Prior to use, the gold electrode was soaked with a mixture solution (98% H_2SO_4: 30% H_2O_2) with a volume ratio of 3:1 for 5 min (*Caution: Piranha solution reacts violently with organic matter!*). Subsequently, it was washed with double-distilled water and carefully dealt with P3000 and P5000 silicon carbide paper. The electrode was then polished to a mirror-like surface with alumina slurries (1, 0.3, 0.05 μm) respectively, followed by rinsing thoroughly with water. After that, it was ultrasonicated with both ethanol and double-distilled water for 5 min. Then, it was electrochemically treated with 0.5 M H_2SO_4 to eliminate any remaining material. Afterward, the electrode was allowed to dry with nitrogen and further immersed with 20 μM peptide solution (20 mM HEPES, 10 mM TCEP, pH 7.0) at room temperature for 16 h. Then, it was soaked in 1 mM MCH for 30 min to resist nonspecific binding on the electrode surface. After thoroughly washed with double-distilled water and dried with nitrogen, the peptide modified electrode was prepared for the PSA experiments.

2.3 GO/AgNPs for signal generation

In order to carry out excellent signal detection process, the reaction conditions for the formation of GO/AgNPs nanocomposites were optimized including reaction temperature and incubation time. Generally, 100 μL of $AgNO_3$ (20.0 mM), 600 μL of GO suspension (1.0 mg mL^{-1}) and 700 μL of ultrapure water were mixed thoroughly at an ambient condition. Subsequently, NaOH was added to adjust the pH value close to 8.0. The reaction temperature was tried from 0 ºC to 80 ºC, and reaction time was in the range from 0 min to 120 min, respectively.

2.4 Fabrication of the PSA biosensor

After modified with thiol-terminated peptide, the electrode was incubated with 200 μL of PSA standard solution of different concentrations for 30 min at 37 °C. In the presence of PSA, peptide can be specifically recognized and cleaved. Then, the electrode was washed with PBS solution for three times (5 min each) to remove any residual protein. The electrode was incubated with 1.0 mg mL^{-1} GO solution for 1 h at room temperature. Primary peptide was conjugated with GO through aromatic amino acids as a linker and GO was self-assembled onto the surface [22], which greatly increases the effective area and conductivity of the electrode. After the electrode was entirely washed with ultrapure water, silver-deposition enhancement was performed by reacting with $AgNO_3$ solution (pH=8.0) at 60°C for 1 h on the electrode surface. AgNPs were immobilized stably through the reduction reaction between GO and Ag^+. After each step, the modified electrode was tested by electrochemical method for the characterization of the fabrication process of the biosensor.

2.5 Electrochemical measurement

Electrochemical impedance spectroscopy (EIS), cyclic voltammetry (CV) and linear sweep voltammetry (LSV) measurements were realized through a CHI660D electrochemical workstation (Shanghai, Chnia). All electrochemical experiments were performed in a conventional three-electrode system that including an Ag/AgCl as the reference electrode, a platinum wire as the counter electrode and a bare or modified gold electrode as the working electrode. EIS and CV measurements were carried out in 5 mM $[Fe(CN)_6]^{3-/4-}$ buffer with 1 M KCl. The EIS parameters were 0.232V biasing potential, 5 mV amplitude, and frequency range of 0.1 Hz - 100 kHz. CV was measured by scanning the potential from -0.3 to +0.7 V, with the scan rate of 50 mV/s. The measurement of LSV was performed in 0.1 M KCl solution with the scanning rate of 50 mV/s.

3. Results and discussion

3.1 Sensing principle

Detailed sensing principle of the peptide-cleavage based electrochemical method for the detection of PSA is illustrated in Scheme 1. The substrate peptide is firstly immobilized on the gold electrode surface via the cysteine at the N terminal [23, 24]. Graphene oxide (GO) is then modified on the electrode surface by the interaction with benzene ring moiety of aromatic amino acids of the peptide. GO possesses large surface area, excellent conductivity, and high stability, which is suitable for electrochemical analysis. In addition, the fascinating electrocatalytic activity of GO helps continuous deposition of silver. Silver ions are firstly absorbed through the uniform functional groups on the basal plane and edges of GO which provide multiple binding sites by electrostatic interactions. Further, numerus silver nanoparticles (AgNPs) are facilely synthesized with GO as the reducing agent and dispersant agent; meanwhile, significant silver

stripping current of AgNPs is obtained, which stands for a highly characteristic solid-state Ag/AgCl reaction [25, 26]. The nanocomposites also have good conductivity to improve the electronic transport efficiency, which could further enhance the final signal. For PSA analysis, the information of PSA concentration is firstly converted to the cleavage of substrate peptide on the electrode surface. Since the cracked peptide can no longer assist the immobilization of GO and subsequent AgNPs, the electrochemical response changes remarkably, which can be used to indicate initial PSA level.

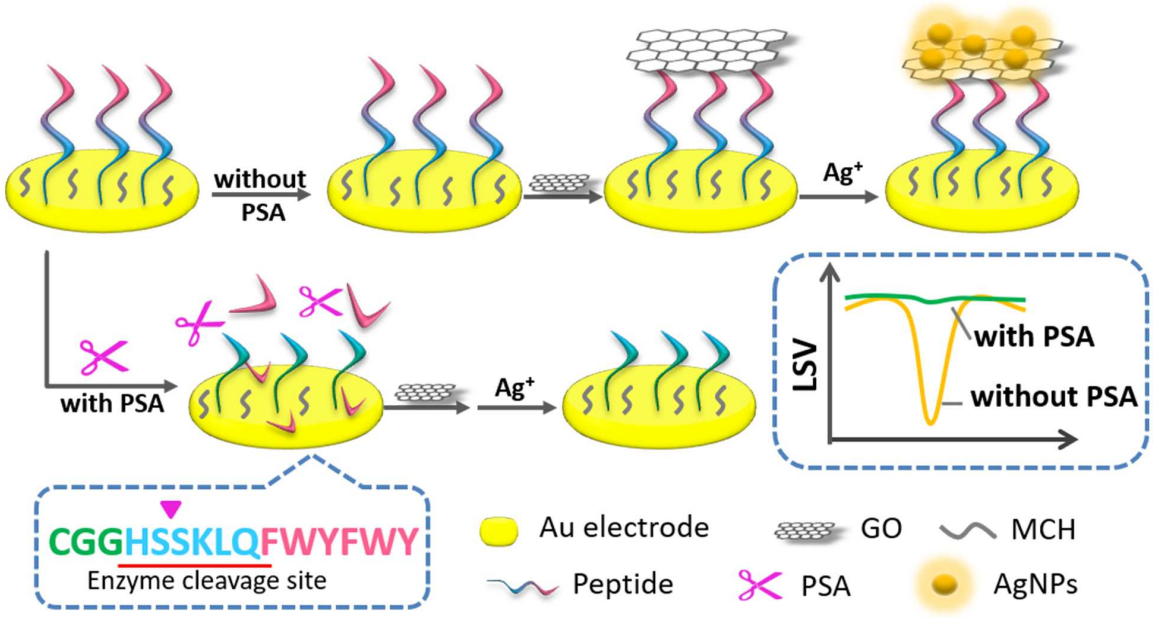

Scheme 1. Illustration of the peptide cleavage-based electrochemical biosensor for the detection of PSA.

3.2 Characterization of GO/AgNPs

The transmission electron microscopy (TEM) images of GO, mixture of GO and Ag^+, GO/AgNPs are recorded, which confirm the successful synthesis of the nanocomposites.

Morphology of GO can be clearly observed. Ag^+ cannot be reduced to AgNPs by preliminarily mixing GO and Ag^+ (Figure 1a to c). The three nanocomposites are then characterized and compared by UV-vis spectra. As shown in Figure 1d, the spectrum of GO/AgNPs exhibits an obvious peak around 400 nm, which confirms that Ag^+ has be reduced to AgNPs. The energy dispersive X-ray spectroscopy further illustrates the element compositions of the nanocomposites, in which carbon, oxygen, and silver element are found (Figure S1).

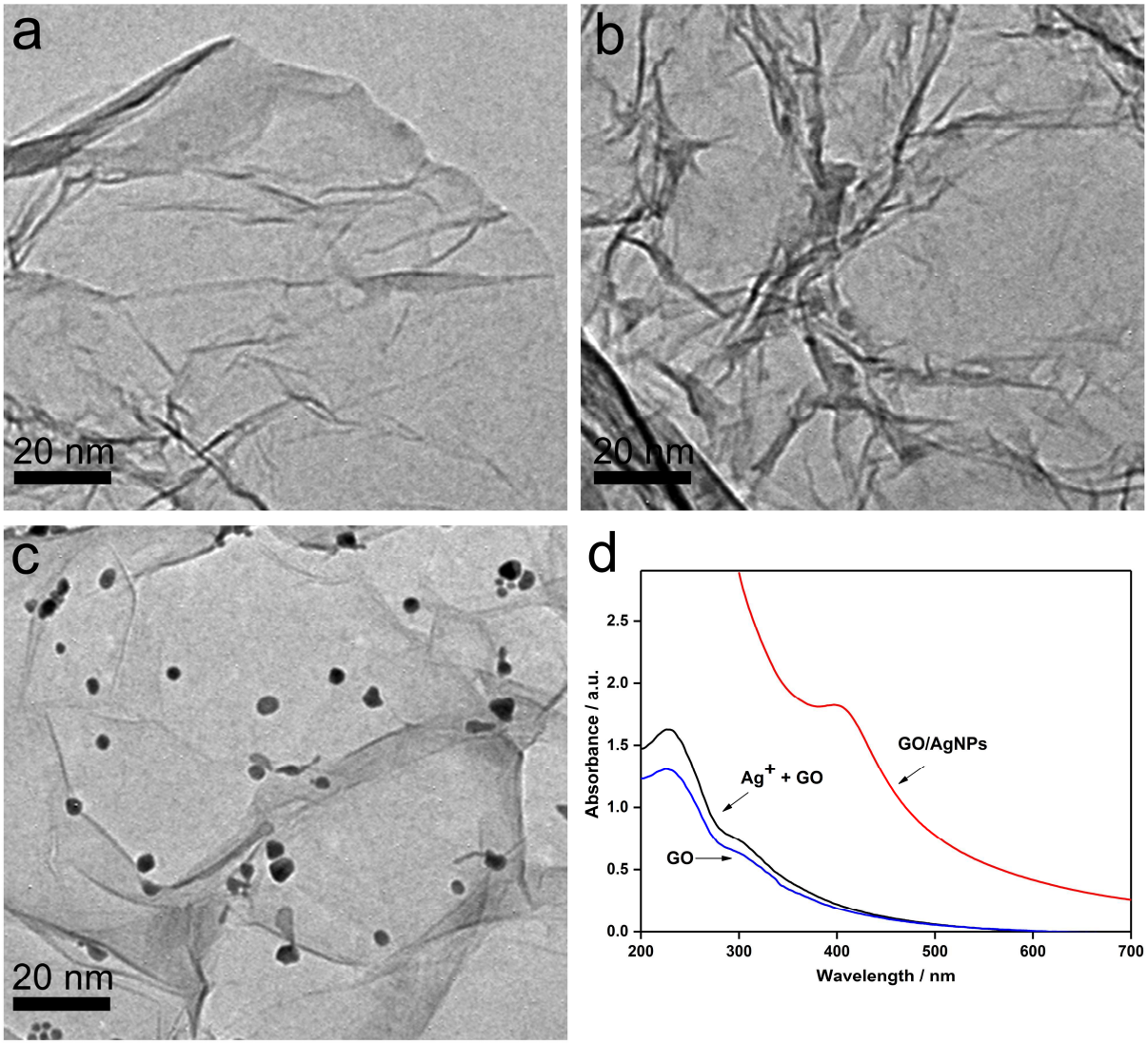

Figure 1. TEM images of (a) GO, (b) GO/Ag^+, (c) GO/AgNPs formed after reacting at 60°C for 1 h. (d) UV-vis absorption spectra of GO, mixture of Ag^+ and GO, GO/AgNPs, respectively.

3.3 Optimization of the synthesis conditions of GO/AgNPs

The reaction time and temperature can significantly affect the reducibility of GO. Therefore, different experiments conditions are tested to obtain optimized conditions for the synthesis of GO/AgNPs. The UV–vis spectra of GO/AgNPs nanocomposites synthesized in alkaline solution with different time are compared (Figure S2a). With the increase of incubation time, the absorbance intensity at 400 nm increases rapidly in the first 30 min and reaches a plateau after 1 h, indicating the reduction reaction is nearly completed (Figure S2b). The reaction temperature is also optimized by UV–vis spectra experiments. The absorbance intensity at 400 nm is continuously enhanced with the temperature from 0 to 80°C, which reveals that higher temperature contributes to the production of more AgNPs (Figure S2c and d). In this study, the reaction time and temperature are set to be 1 h and 60 °C for good yield and mild reaction conditions.

3.4 Characterization of the electrode

To efficiently characterize the interface properties of the modified electrode, the assembly processes have been monitored by EIS measurement in which $[Fe(CN)_6]^{3-/4-}$ is used as the electroactive probe. For a typical Nyquist plot, the equivalent circuit model of the working electrode is applied and the semicircle diameter of impedance increases with the constant blocking by the transfer of redox probe. As is shown in Figure 2, the curve of bare gold electrode is almost a straight line without obvious semicircular domain, indicating that surface electrons transfer directly. When the sulfhydryl-terminal peptide is immobilized on the electrode, the

impedance increases due to the attenuation of electron transfer by peptide. Since aromatic amino acids of the peptide could interact with benzene rings of GO, the negatively charged 2-D nanosheets could be easily assembled on the electrode, which leads to further increase of the impedance caused by the significant repellent between GO and $[Fe(CN)_6]^{3-/4-}$. However, after subsequent formation of AgNPs, the impendence value is decreased sharply, which is due to the fact that the formed AgNPs could effectively promote electron transfer. Therefore, the stepwise variation of impedance value confirms the successful fabrication of the biosensor.

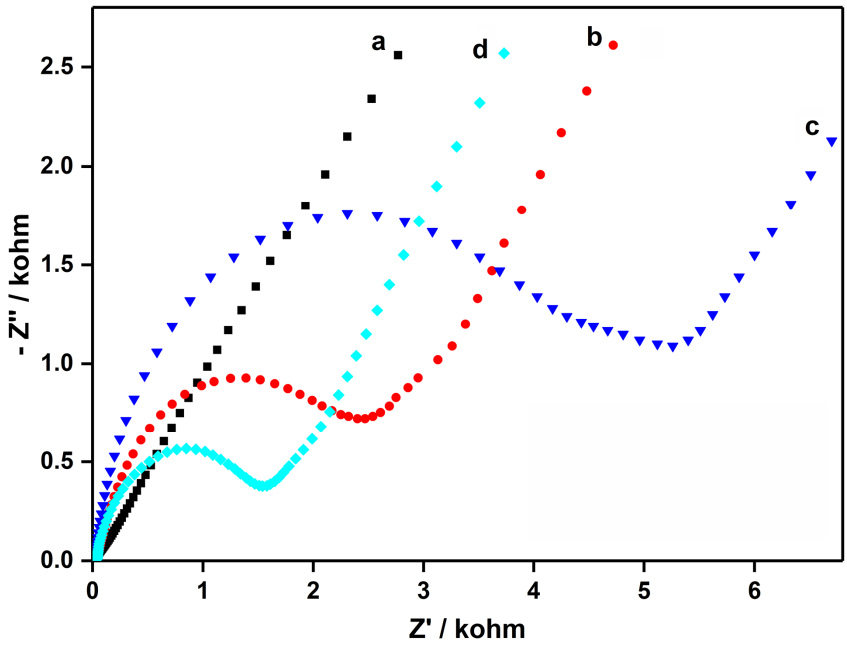

Figure 2. Nyquist diagrams of (a) bare gold electrode, (b) after modified with peptide, (c) after GO assembly and (d) further silver deposition.

3.5 Optimization of the experimental conditions

In order to demonstrate the appropriate concentration of the immobilized peptide, CV measurements are performed. A pair of well-defined redox peaks of $[Fe(CN)_6]^{3-/4-}$ is obtained at

a bare gold electrode. After disparate levels of peptide are modified on the electrode, the peak current decreases gradually with the increase of peptide (Figure S3a and b). After reaching 20 μM, the peak tends to be stable. Thus, 20 μM peptide is selected for the further experiments. PSA cleavage time is another important parameter affecting the analytical performance of the biosensor, the effect of which is also investigated by CV. The peak current corresponding to PSA (1 ng mL^{-1}) cleavage increases consistently with the reaction time up to 30 min, which reveals the reaction is nearly finished (Figure S3c and d).

3.6 Analytical performance of the PSA biosensor.

GO with huge surface area facilitates the loading of numerous AgNPs, which may provide significant electrochemical responses. LSV is applied to evaluate silver stripping peaks after treated with different amount of target PSA. As shown in Figure 3, under optimum conditions, the peak current decreases with the increasing concentration of PSA. The corresponding calibration curve shows a good linear relationship between the peak current and the logarithm of the PSA concentration ranging from 5 pg·mL^{-1} to 20 ng·mL^{-1}. The fitting equation is

$$y = -0.6595 \log x + 3.4154 \ (n = 3, R^2 = 0.993)$$

in which, x is the concentration of PSA (pg·mL^{-1}), y stands for the peak current (10^{-4}A). The limit of detection (LOD) for PSA analysis is calculated to be 0.33 pg mL^{-1} at 3σ, which is quite low. The wide linear range and high sensitivity provides powerful evidences of the proposed strategy for highly sensitive and effective detection of PSA. The analytical performances are excellent compared with currently developed methods for PSA assay (Table 1).

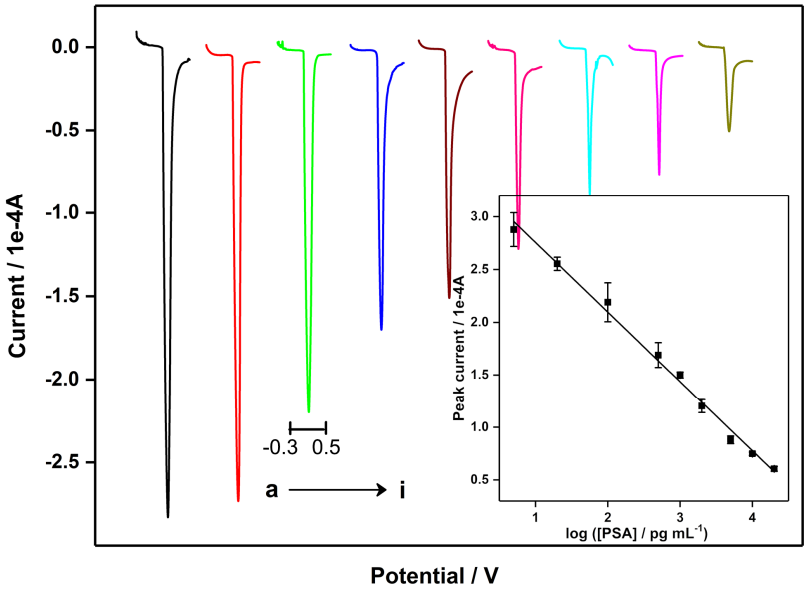

Figure 3. Linear sweep voltammograms for the detection of PSA with the concentrations of (a-i) 5 pg mL^{-1}, 20 pg mL^{-1}, 100 pg mL^{-1}, 500 pg mL^{-1}, 1 ng mL^{-1}, 2 ng mL^{-1}, 5 ng mL^{-1}, 10 ng mL^{-1}, 20 ng mL^{-1}. Inset shows the calibration curve reflecting the linear relationship between logarithmic concentration of PSA and peak current.

Table 1. Analytical performance comparison of this work with other reported PSA assays.

Technique	Strategy	Detection range (pg mL^{-1})	LOD (pg mL^{-1})	Ref
cyclic voltammetry	epitope binning assay	-	5×10^{5}	[27]
reflectance spectroscopy	white light reflectance spectroscopy biosensing system	5×10^{2} to 5×10^{5}	500	[28]
particle	microwell-based microbead	1.25×10^{2} to	125	[29]

analysis system	aggregation assay	2.5×10^5		
SWV	aptamer based biosensor	80 to 10^5	80	[30]
velocimetry	bead-based immunosensing with nanofluidic preconcentration	0 to 3.2×10^6	50	[31]
DPV	hemin functionalized graphene-conjugated palladium nanocomposites	25 to 2.05×10^5	8	[32]
SWV	biotinylated-antibody/cyclodextrin inclusion complex	10 to 2.5×10^4	6.7	[33]
Photoelectrochemical assay	Carbon Dots/g-C_3N_4 nanoheterostructures and copper nanoclusters	20 to 10^5	5	[34]
LSV	peptide and GO/AgNPs	5 to 2×10^4	0.33	this work

3.7 Selectivity investigation

The specificity of the electrochemical biosensor is due to the peptide sequence, which can be cleaved only in the presence of PSA. We have introduced a random peptide sequence to investigate the effect of peptide sequence. The random peptide modified electrode does not respond to target PSA (5 pg mL^{-1}), while in the case of specific peptide, the peak intensity decreases significantly, which is due to the specific recognition of PSA and the subsequent

cleavage (Figure S4). To evaluate the selectivity of the electrochemical biosensor, it has been challenged with other possible interferences such as CEA, AFP, and BSA in the same conditions. The obtained results are exhibited in Figure 4. When the biosensor is incubated with the interfering proteins with relatively higher concentrations, no apparent changes of the current are observed compared to the blank test, which demonstrate that the designed peptide cannot be cleaved by these proteins. Only in the presence of PSA, specific cleavage reaction occurs, which inhibits the subsequent GO immobilization of silver deposition. The finally obtained peak currents are remarkably decreased. All these results confirms the proposed biosensor has a good specificity for PSA analysis.

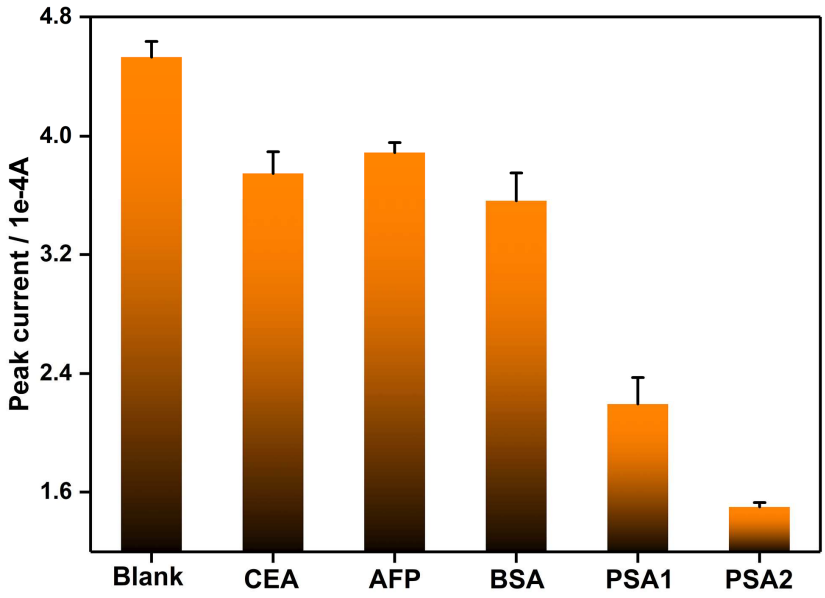

Figure 4. Selectivity investigation of the proposed PSA (PSA1: 100 pg mL^{-1}; PSA2: 1 ng mL^{-1}) assay against other interfering proteins (1 ng mL^{-1}).

3.8 Analysis of clinical serum specimens

We have further evaluated the recoveries of standard PSA spiked in independent healthy human serum samples by the proposed method. The results are listed in Table 2. The detected values are similar with initially added values. The recoveries are in the range from 83.4% to 106.7%, which are quite satisfactory. Therefore, this method may have a promising potential application for the detection of PSA in clinical analysis.

Table 2. Analytical results of PSA in clinical serum samples.

Sample	Spiked (ng mL^{-1})	Detected (ng mL^{-1})	Recovery (%)
Serum 1	2.0	1.995	99.8%
	5.0	4.365	87.3%
Serum 2	2.0	2.037	101.9%
	5.0	4.168	83.4%
Serum 3	2.0	2.133	106.7%
	5.0	4.265	85.3%

CONCLUSIONS

In summary, with target-induced cleavage of peptide, a novel electrochemical biosensor for sensitive detection of PSA has been successfully constructed. By employing GO/AgNPs nanocomposites, wide liner range and low detection limit are achieved. The excellent performances of the proposed biosensor should be attributed to the following reasons. First, a short peptide is used to replace traditional antibodies for PSA recognition due to its good stability, reaction efficiency, and the ability to accommodate different environments; Second, GO/AgNPs enhancement improves the precision and sensitivity of the detection. In view of the

above advantages, we anticipate that this highly sensitive and selective method has great potential to be applied in clinical applications.

Acknowledgments

This work is supported by the National Natural Science Foundation of China (Grant No. 81771929 and 81671779), the Natural Science Foundation of Tianjin (Grant No. 17JCQNJC13900), the Key Projects of Tianjin Science and Technology Support Program (Grant No. 16YFZCSY00440) and Science and Technology Development Program of Jilin (Grant No. 20180201061YY).

Supplementary data

Supplementary data can be found in the online version.

REFERENCES

[1] J. Cooley, T.K. Takayama, S.D. Shapiro, N.M. Schechter, E. Remold-O'Donnell, The serpin MNEI inhibits elastase-like and chymotrypsin-like serine proteases through efficient reactions at two active sites, Biochemistry, 40 (2001) 15762-15770.

[2] S.P. Balk, Y.J. Ko, G.J. Bubley, Biology of prostate-specific antigen, J. Clin. Oncol., 21 (2003) 383-391.

[3] G. Attard, C. Parker, R.A. Eeles, F. Schroder, S.A. Tomlins, I. Tannock, C.G. Drake, J.S. de Bono, Prostate cancer, Lancet, 387 (2016) 70-82.

[4] T. Maurer, M. Eiber, M. Schwaiger, J.E. Gschwend, Current use of PSMA - PET in prostate cancer management, Nat. Rev. Urol., 13 (2016) 226-235.

[5] G.C. Fan, X.M. Shi, J.R. Zhang, J.J. Zhu, Cathode photoelectrochemical immunosensing platform integrating photocathode with photoanode, Anal. Chem., 88 (2016) 10352-10356.

[6] C. Ibau, M.K.M. Arshad, S.C.B. Gopinath, Current advances and future visions on bioelectronic immunosensing for prostate-specific antigen, Biosens. Bioelectron., 98 (2017) 267-284.

[7] D.A. Healy, C.J. Hayes, P. Leonard, L. McKenna, R. O'Kennedy, Biosensor developments: application to prostate-specific antigen detection, Trends Biotechnol., 25 (2007) 125-131.

[8] W.Q. Lai, D.P. Tang, J.Y. Zhuang, G.N. Chen, H.H. Yang, Magnetic bead-based enzyme-chromogenic substrate system for ultrasensitive colorimetric immunoassay accompanying cascade reaction for enzymatic formation of squaric acid-iron(III) chelate, Anal. Chem., 86 (2014) 5061-5068.

[9] B.X. Li, J. Liu, H. Zhou, Amplified fluorescence detection of serum prostate specific antigen based on metal-dependent DNAzyme assistant nanomachine, Anal. Chim. Acta, 1008 (2018) 96-102.

[10] Y.Y. Zhang, X.P. Wang, S. Pemer, A. Bankfalvi, S. Schlucker, Effect of antigen retrieval methods on nonspecific binding of antibody-metal nanoparticle conjugates on formalin-fixed paraffin-embedded tissue, Anal. Chem., 90 (2018) 760-768.

[11] X.Q. Chen, G.B. Zhou, P. Song, J.J. Wang, J.M. Gao, J.X. Lu, C.H. Fan, X.L. Zuo, Ultrasensitive electrochemical detection of prostate-specific antigen by using antibodies anchored on a DNA nanostructural scaffold, Anal. Chem., 86 (2014) 7337-7342.

[12] Y.L. Wang, F.R. Liu, J.T. Cao, S.W. Ren, Y.M. Liu, Spatial-resolved dual-signal-output electrochemiluminescent ratiometric strategy for accurate and sensitive immunoassay, Biosens. Bioelectron., 102 (2018) 525-530.

[13] P. Miao, Y.T. Jiang, Y.H. Wang, J. Yin, Y.G. Tang, An electrochemical approach capable of prostate specific antigen assay in human serum based on exonuclease-aided target recycling amplification, Sens. Actuator B-Chem., 257 (2018) 1021-1026.

[14] E. Wonder, L. Simon-Gracia, P. Scodeller, R.N. Majzoub, V.R. Kotamraju, K.K. Ewert, T. Teesalu, C.R. Safinya, Competition of charge-mediated and specific binding by peptide-tagged cationic liposome-DNA nanoparticles in vitro and in vivo, Biomaterials, 166 (2018) 52-63.

[15] F.Y. Meng, W.G. Liang, H.X. Sun, L.G. Wu, X. Gong, P. Miao, A peptide-based electrochemical biosensor for facile measurement of whole-blood heparin, ChemElectroChem, 4 (2017) 472-475.

[16] H. Lee, Y. Park, S. Kim, Enzymatic cross-linking of side chains generates a modified peptide with four hairpin-like bicyclic repeats, Biochemistry, 56 (2017) 4927-4930.

[17] J. Wang, M. Muto, R. Yatabe, Y. Tahara, T. Onodera, M. Tanaka, M. Okochi, K. Toko, Highly selective rational design of peptide-based surface plasmon resonance sensor for direct determination of 2,4,6-trinitrotoluene (TNT) explosive, Sens. Actuator B-Chem., 264 (2018) 279-284.

[18] P. Miao, J. Yin, L.M. Ning, X.X. Li, Peptide-based electrochemical approach for apoptosis evaluation, Biosens. Bioelectron., 62 (2014) 97-101.

[19] V.R. Rodovalho, G.R. Araujo, E.R. Vaz, C. Ueira-Vieira, L.R. Goulart, J.M. Madurro, A.G. Brito-Madurro, Peptide-based electrochemical biosensor for juvenile idiopathic arthritis detection, Biosens. Bioelectron., 100 (2018) 577-582.

[20] F.F. Wu, Y. Zhou, H. Zhang, R. Yuan, Y.Q. Chai, Electrochemiluminescence peptide-based biosensor with hetero-nanostructures as coreaction accelerator for the ultrasensitive determination of tryptase, Anal. Chem., 90 (2018) 2263-2270.

[21] S.R. Denmeade, W. Lou, J. Lovgren, J. Malm, H. Lilja, J.T. Isaacs, Specific and efficient peptide substrates for assaying the proteolytic activity of prostate-specific antigen, Cancer Res., 57 (1997) 4924-4930.

[22] J. Zhou, X.H. Xu, W. Liu, X. Liu, Z. Nie, M. Qing, L.H. Nie, S.Z. Yao, Graphene oxide-peptide nanocomplex as a versatile fluorescence probe of protein kinase activity based on phosphorylation protection against carboxypeptidase digestion, Anal. Chem., 85 (2013) 5746-5754.

[23] Y.J. Yu, Q. Zhang, J. Buscaglia, C.C. Chang, Y. Liu, Z.H. Yang, Y.C. Guo, Y.T. Wang, K. Levon, M. Rafailovich, Quantitative real-time detection of carcinoembryonic antigen (CEA) from pancreatic cyst fluid using 3-D surface molecular imprinting, Analyst, 141 (2016) 4424-4431.

[24] Y.J. Yu, Q. Zhang, C.C. Chang, Y. Liu, Z.H. Yang, Y.C. Guo, Y.T. Wang, D.K. Galanakis, K. Levon, M. Rafailovich, Design of a molecular imprinting biosensor with multi-scale roughness for detection across a broad spectrum of biomolecules, Analyst, 141 (2016) 5607-5617.

[25] Y.P. Dou, J.J. Peng, W. Li, M. Li, H.H. Liu, H.M. Zhang, Effects of reducibility of graphene oxide nanosheets on preparation of AgNPs/GO nanocomposites and their electrocatalytic performance, J. Nanopart. Res., 17 (2015) 489.

[26] J. Wang, J. Yu, X.Y. Zhou, P. Miao, Exonuclease and nicking endonuclease-assisted amplified electrochemical detection of coralyne, ChemElectroChem, 4 (2017) 1828-1831.

[27] M. Li, X.D. Guo, H. Li, X.L. Zuo, R.Z. Hao, H.B. Song, A. Aldalbahi, Z.L. Ge, J. Li, Q. Li, S.P. Song, S.H. Li, N.S. Shao, C.H. Fan, L.H. Wang, Epitope binning assay using an electron transfer-modulated aptamer sensor, ACS Appl. Mater. Interfaces, 10 (2018) 341-349.

[28] G. Koukouvinos, A. Metheniti, C.E. Karachaliou, D. Goustouridis, E. Livaniou, K. Misiakos, I. Raptis, A. Kondili, P. Miniati, P. Petrou, S. Kakabakos, White light reflectance spectroscopy biosensing system for fast quantitative prostate specific antigen determination in forensic samples, Talanta, 175 (2017) 443-450.

[29] W.W. Cui, M.H. He, L.Y. Mu, Z.Z. Lin, Y.Y. Wang, W. Pang, M. Reed, X.X. Duan, Cellphone-enabled microwell-based microbead aggregation assay for portable biomarker detection, ACS Sens., 3 (2018) 432-440.

[30] B.P. Crulhas, A.E. Karpik, F.K. Delella, G.R. Castro, V.A. Pedrosa, Electrochemical aptamer-based biosensor developed to monitor PSA and VEGF released by prostate cancer cells, Anal. Bioanal. Chem., 409 (2017) 6771-6780.

[31] Y.J. Fan, C.Z. Deng, P.S. Chung, W.C. Tian, H.J. Sheen, A high sensitivity bead-based immunoassay with nanofluidic preconcentration for biomarker detection, Sens. Actuator B-Chem., 272 (2018) 502-509.

[32] G.J. Zhang, Z.G. Liu, L.F. Fan, Y.J. Guo, Electrochemical prostate specific antigen aptasensor based on hemin functionalized graphene-conjugated palladium nanocomposites, Microchim. Acta, 185 (2018) 159.

[33] M.F. Mousavi, M. Amiri, A. Noori, S.M. Khoshfetrat, A prostate specific antigen immunosensor based on biotinylated-antibody/cyclodextrin inclusion complex: fabrication and electrochemical studies, Electroanalysis, 29 (2017) 2818-2831.

[34] S.Z. Lv, Y. Li, K.Y. Zhang, Z.Z. Lin, D.P. Tang, Carbon dots/g-C3N4 nanoheterostructures-based signal-generation tags for photoelectrochemical immunoassay of cancer biomarkers coupling with copper nanoclusters, ACS Appl. Mater. Interfaces, 9 (2017) 38336-38343.

Table 1. Analytical performance comparison of this work with other reported PSA assays.

Technique	Strategy	Detection range (pg mL^{-1})	LOD (pg mL^{-1})	Ref
cyclic voltammetry	epitope binning assay	-	5×10^5	[27]
reflectance spectroscopy	white light reflectance spectroscopy biosensing system	5×10^2 to 5×10^5	500	[28]
particle analysis system	microwell-based microbead aggregation assay	1.25×10^2 to 2.5×10^5	125	[29]
SWV	aptamer based biosensor	80 to 10^5	80	[30]
velocimetry	bead-based immunosensing with nanofluidic preconcentration	0 to 3.2×10^6	50	[31]
DPV	hemin functionalized graphene-conjugated palladium nanocomposites	25 to 2.05×10^5	8	[32]
SWV	biotinylated-antibody/cyclodextrin inclusion complex	10 to 2.5×10^4	6.7	[33]
Photoelectrochemical assay	Carbon Dots/g-C_3N_4 nanoheterostructures and copper nanoclusters	20 to 10^5	5	[34]
LSV	peptide and GO/AgNPs	5 to 2×10^4	0.33	this work

Table 2. Analytical results of PSA in clinical serum samples.

Sample	Spiked (ng mL^{-1})	Detected (ng mL^{-1})	Recovery (%)
Serum 1	2.0	1.995	99.8%
	5.0	4.365	87.3%
Serum 2	2.0	2.037	101.9%
	5.0	4.168	83.4%
Serum 3	2.0	2.133	106.7%
	5.0	4.265	85.3%